Declined Expression of Histone Deacetylase 6 Contributes to Periodontal Ligament Stem Cell Aging

Qian Li,* Yushi Ma,* Yunyan Zhu,* Ting Zhang,* and Yanheng Zhou*

Background: Identification of regulators for aging-associated stem cell (SC) dysfunctions is a critical topic in SC biology and SC-based therapies. Periodontal ligament stem cell (PDLSC), a kind of dental mesenchymal SC with dental regeneration potential, ages with functional deterioration in both in vivo and ex vivo expansion. However, little is known about regulators for PDLSC aging.

Methods: Expression changes of a potential regulator for PDLSC aging, histone deacetylase 6 (HDAC6), were evaluated within various models. Senescence-associated phenotypic and functional alternations of PDLSC in loss-of-function models for HDAC6 were examined using HDAC6-specific pharmacologic inhibitors or RNA interference-based knockdown. Involvement of $p27^{Kip1}$ in HDAC6-associated aging was demonstrated by its acetylation and stability changes along with overexpression or functional inhibition of HDAC6.

Results: Expression of HDAC6 decreased significantly in replicative senescence and induced SC aging models. Loss-of-function experiments suggested that pharmacologic inhibition of deacetylase activity of HDAC6 accelerated PDLSC senescence and impaired its SC activities, which showed reduced osteogenic differentiation and diminished migration capacities. Examination of markers for proliferative exhaustion of SCs revealed that protein level of $p27^{Kip1}$ was specifically elevated after HDAC6 inhibition. HDAC6 physically interacted with $p27^{Kip1}$ and could deacetylate $p27^{Kip1}$. Importantly, acetylation of $p27^{Kip1}$ was negatively regulated by HDAC6, which correlated with alteration of $p27^{Kip1}$ protein levels.

Conclusion: Data suggest that HDAC6 plays an important role in PDLSC aging, which is dependent, at least partially, on regulation of $p27^{Kip1}$ acetylation. *J Periodontol 2017; 88:e12-e23.*

KEY WORDS

Acetylation; aging; cyclin-dependent kinase inhibitor p27; histone deacetylases; periodontal ligament; proteins; stem cells.

* Department of Orthodontics, Peking University School and Hospital of Stomatology, National Engineering Laboratory for Digital and Material Technology of Stomatology, Beijing Key Laboratory of Digital Stomatology, Beijing, China.

Accumulating damages to various biologic macromolecules leads to universal decline of tissue homeostasis and regeneration during aging, a hallmark of stem cell (SC) exhaustion.[1] Similarly, many ex vivo expanded SCs with the potential for clinical therapies experience age-dependent functional deterioration along with repopulation.[2] As a prototypical adult SC with capacities for differentiation into a broad class of tissues, mesenchymal SCs (MSCs) are developing into a promising therapeutic agent for tissue regeneration. However, application of MSCs is not exempted from such vulnerabilities to senescence, which are believed to be set by both intrinsic factors and environmental niche.[3] Clinical treatment with MSCs from older donors was reported to be less effective than their younger counterparts.[4] These senescent MSCs feature a panel of characteristics, including: 1) morphologically enlarged cell bodies; 2) slow or halted cell proliferation; 3) elevated senescence-associated (SA) β-galactosidase (SA-β-gal) activity; 4) reduced migration capacity; and 5) decreased differentiation potential.[5] Despite various models and markers being proposed to explain or validate the aging state of MSCs, activation of tumor suppressors, such as $p16^{INK4a}$, $p53/p21^{Cip1}$, and $p27^{Kip1}$, is emerging as a pivotal event in cellular senescence and SC degeneration.[5] In this regard, all these proteins were reported to be barriers for induced pluripotency.[6-8]

doi: 10.1902/jop.2016.160338

Periodontal ligament (PDL) SC (PDLSC) is a type of dental MSC isolated from PDL.[9] Besides its basic function to support collagenous fibers in dense connective tissue of teeth, PDLSC is implicated in the maintenance of periodontal homeostasis and replenishment of impaired cells during healing of dental damages. In line with these tissue regeneration capacities, multipotent PDLSCs are able to differentiate into neurogenic, cardiomyogenic, chondrogenic, and osteogenic lineages.[10] Accordingly, cell therapy with PDLSCs is considered to be encouraging for treatment of human periodontitis and other diseases demanding dental regeneration.[11-14] However, a general hindrance against clinical application of PDLSCs is degeneration of SC function of PDLSCs in older individuals or younger ones with prematurely developed age-related conditions.[15] Indeed, the critical value of PDLSCs for osteoblastic differentiation has been reported to be severely compromised in the senescent state after replicative exhaustion or exposure to stress.[16]

Histone deacetylase 6 (HDAC6) is a member of Class IIb HDACs, with a unique duplicated deacetylase domain and ubiquitin-binding domain.[17] HDAC6 is mainly localized in the cytoplasm, and its primary enzymatic targets include α-tubulin, cortactin, and chaperone heat shock protein HSP90α.[18] Hence, HDAC6 is broadly involved in many cellular processes, such as maintenance of cellular shape and polarity, intracellular transport, and directional movement, based on its erasure of acetylation of two key cytoskeletal components: α-tubulin and cortactin.[18] However, compared with its well-defined roles in cancer and neurodegenerative diseases, little is known about its effect on SC aging and cellular senescence.

In this study, HDAC6 is reported to be a critical regulator of PDLSC aging. Decreased expression of HDAC6 is evident in various senescence models including human samples. Inhibition of deacetylase activity of HDAC6 is observed to impair SC function of PDLSCs. Linkage between enzymatic activity of HDAC6 and stability of pivotal senescence protein $p27^{Kip1}$ is demonstrated.

MATERIALS AND METHODS

Cell Lines, Cell Culture, and Treatment

This study was carried out from February 1, 2015, to May 30th, 2016, at Peking University School of Stomatology, Beijing, China. Human cell samples were obtained from the School and Hospital of Stomatology, Peking University, under approved guidelines set by the Peking University Ethical Committee, with oral informed consent from all patients. PDLSCs isolated from donors (three males and two females, aged 13 to 63 years; mean age: 35 years) were cultured according to previously reported protocols with slight modifications.[19,20] PDL tissues were separated from the mid-third of the root surface and minced into small tissue cubes. Tissue cubes were digested with 3 mg/mL collagenase (Type I)† with 4 mg/mL dispase‡ in α-minimum essential medium (α-MEM)§ for 15 minutes at 37°C with vigorous shaking. Tissue explants were plated into culture dishes containing α-MEM supplemented with 10% fetal bovine serum (FBS),‖ 0.292 mg/mL glutamine,¶ 100 units/mL penicillin streptomycin,# and 100 μM ascorbic acid** and further incubated at 37°C in a humidified atmosphere containing 5% CO_2. Gingival SCs (GMSCs) and dental pulp SCs (DPSCs) were acquired similarly but from gingiva or dental pulp, respectively. For DNA damage-induced senescence, PDLSCs at passage 2 (P2) from a 30-year-old donor were treated with 10 μM etoposide (ETO)†† for 48 hours; α-MEM was replaced with fresh medium, and cells were further cultivated for 6 days. To attain replicative exhaustion, continuous culturing of PDLSCs at P2 from a 30-year-old donor was performed to reach a morphologic senescence state. For pharmacologic HDAC6 inhibition, rocilinostat‡‡ and tubastatin A§§ were used at concentrations of 5 μM each.

Flow Cytometric Analysis of Isolated PDLSCs

To validate the identity of isolated PDLSCs, flow cytometry was used to examine representative surface markers, including CD45, CD34, CD29, CD90, CD73, and CD146. Aliquots of PDLSCs ($>2 \times 10^5$) were fixed with 4% paraformaldehyde, followed by suspension in phosphate-buffered saline (PBS) supplemented with 3% FBS and primary antibodies against normal immunoglobulin G, CD45, CD34, CD29, CD73, CD90, or CD146.‖‖ After incubation for 1 hour at 4°C in the dark, cells were washed and incubated with secondary fluorescent antibodies for 45 minutes at room temperature. Cell suspensions without antibodies served as matched controls. Samples were analyzed with a flow cytometer using an analysis program according to the manufacturer.¶¶

Measurement of SA Phenotypes

For the SA-β-gal staining experiment, cells fixed with formaldehyde were incubated in freshly prepared SA-β-gal staining solution at 37°C overnight followed by examination with photomicrography as described previously.[21] For colony formation assay, 3×10^3 cells were seeded on six-well plates. After selection, cells were fixed with formaldehyde and stained with

† Sigma-Aldrich, St. Louis, MO.
‡ Sigma-Aldrich.
§ HyClone, GE Healthcare Life Sciences, Pittsburgh, PA.
‖ HyClone, GE Healthcare Life Sciences.
¶ HyClone, GE Healthcare Life Sciences.
# HyClone, GE Healthcare Life Sciences.
** Sigma-Aldrich.
†† Sigma-Aldrich.
‡‡ Selleck Chemicals, Houston, TX.
§§ Selleck Chemicals.
‖‖ BD Biosciences, San Jose, CA.
¶¶ BD Biosciences.

crystal violet.[##] For 3-(4,5-dimethylthiazol-2-yl)-2,5-diphenyltetrazolium bromide (MTT) assay, cells were seeded into 96-well plates at a density of 2×10^3 cells/well. Aliquot of cells was stained with 20 μL of MTT[***] (10 μg/mL in PBS) for 3 hours and quantified by spectrophotometry every 24 hours. For 5-bromo-2′-deoxyuridine (BrdU) incorporation analysis, cells were incubated at 37°C in presence of 10 μM BrdU for 4 hours, followed by fixation, permeabilization, denaturation, and blocking. Immunostaining was performed using antibodies against BrdU.[†††] Cells positive for BrdU were counted under a fluorescence microscope.[‡‡‡]

Transwell Assay and Scratch Assay

Transwell assay was performed in a Boyden chamber. PDLSCs ($\approx 1 \times 10^4$) in the upper chamber were maintained in medium without serum, whereas medium containing 10% FBS was kept in the lower chamber with a chemoattractant function. After 24 hours of incubation, cells that could not penetrate membranes were wiped out. Resulting membranes were fixed followed by staining with 0.5% crystal violet, and were examined using an inverted microscope.[§§§] Scratch assay was performed on the monolayer of PDLSCs at confluence, which was wounded by a micropipette tip. The wound healing process was monitored by photomicrography in a 24-hour interval.

Coimmunoprecipitation (CoIP) and Western Blotting Analyses

For CoIP assay, cells were collected and lysed on ice with lysis buffer containing 0.5% non-ionic detergent.[‖‖] Lysates were precleared by incubation with protein A beads.[¶¶¶] Protein complex was precipitated with a specific antibody (anti-$p27^{Kip1}$[###] or anti-HDAC6[****]) conjugated with protein A beads followed by extensive washing. Resulting materials were analyzed by western blotting. For measurement of $p27^{Kip1}$ acetylation, FLAG-$p27^{Kip1}$ was purified by resin conjugated with antibodies against FLAG[††††] and eluted from beads with excessive competitive FLAG peptide.[‡‡‡‡] Western blotting analyses were performed as previously described.[21] Antibodies for HDAC6,[§§§§] $p27^{Kip1}$,[‖‖‖] GAPDH,[¶¶¶¶] $p16^{INK4a}$,[####] $p21^{Cip1}$,[*****] FLAG,[†††††] and pan-acetylation[‡‡‡‡‡] were used in this study.

Osteogenic Differentiation and Alizarin Red Staining (ARS) Assay

PDLSCs were cultured in standard medium until they reached subconfluence. Medium was switched to osteogenic differentiation media containing 10% FBS, 50 mg/mL ascorbic acid, 10 nM dexamethasone, and 10 mM β-glycerophosphate. PDLSCs were further cultured for 3 weeks.[22] Medium was changed every 3 days. PDLSCs were fixed and incubated with staining buffer containing alizarin red[§§§§§] followed by visualization using photomicrography.

Quantitative Reverse-Transcription Polymerase Chain Reaction (qRT-PCR)

Total cellular RNAs were isolated[‖‖‖‖] to serve as a template for first-strand complementary DNA synthesis using a reverse transcription system.[¶¶¶¶¶] Quantitation of all gene transcripts was performed by quantitative PCR[#####] with expression of *GAPDH* as internal control. Primers used for qRT-PCR are as listed: 1) *HDAC6* forward (F): tttcaactctgtggctgtgg, *HDAC6* reverse (R): tgtgctgagttccattaccg; 2) *alkaline phosphatase* (*ALP*) F: tgttcgtcatgggtgtgaac, *ALP* R: gttgtcatggatgaccttgg; 3) *collagen Type 1 alpha 1 (Col1A1)* F: ttctgcaacatggagactgg, *Col1A1* R: aatccatcggtcatgctctc; 4) *bone morphogenetic protein 4 (BMP4)* F: tccacagcactggtcttgag, *BMP4* R: atgttcttcgtggtggaagc; 5) *CCNA2* F: gaatgagaccctgcatttgg; *CCNA2* R: gcccacaagctgaagttttc; 6) $p16^{INK4a}$ F: GAAGGTCCCTCAGACATCCCC; $p16^{INK4a}$ R: CCCTGTAGGACCTTCGGTGAC; 7) $p21^{Cip1}$ F: atgtggacctgtcactgtcttg, $p21^{Cip1}$ R: aatctgtcatgctggtctgc; 8) $p27^{Kip1}$ F: catttggtggacccaaagac, $p27^{Kip1}$ R: tgcaggtcgcttccttattc; and 9) *GAPDH* F: tgttcgtcatgggtgtgaac, *GAPDH* R: gttgtcatggatgaccttgg.

Plasmids and Small Interference RNA (siRNA) Transfection

Plasmids were transiently transfected into cells at 70% to 80% confluence with transfection reagent[******] following instructions of the manufacturer. Targeting sequences of siRNA[††††††] were synthesized as follows: siRNA against HDAC6 (siHDAC6), GUGGCCGCAUUAUCCUUAU; non-silencing control (siNC), UUCUCCGAACGUGUCACGU. Transfections of siRNAs were performed using a reagent[‡‡‡‡‡‡] according to the instructions of the manufacturer.

Materials

##	Sigma-Aldrich.
***	Sigma-Aldrich.
†††	BD Biosciences.
‡‡‡	Carl Zeiss Microscopy, Jena, Germany.
§§§	Olympus, Tokyo, Japan.
‖‖‖	NP-40, AMRESCO, OH.
¶¶¶	Sigma-Aldrich.
###	Santa Cruz Biotechnology, Dallas, TX.
****	Proteintech, Rosemont, IL.
††††	Sigma-Aldrich.
‡‡‡‡	Sigma-Aldrich.
§§§§	HyClone, GE Healthcare Life Sciences.
‖‖‖‖	Santa Cruz Biotechnology.
¶¶¶¶	Santa Cruz Biotechnology.
####	Santa Cruz Biotechnology.
*****	Santa Cruz Biotechnology.
†††††	Sigma-Aldrich.
‡‡‡‡‡	Proteintech.
§§§§§	Sigma-Aldrich.
‖‖‖‖‖	RNeasy Mini Kit, Qiagen, Venlo, The Netherlands.
¶¶¶¶¶	Promega, Madison, WI.
#####	ABI PRISM 7500 sequence detection system, Applied Biosystems, Thermo Fisher Scientific, Waltham, MA.
******	Lipofectamine 3000, Invitrogen, Thermo Fisher Scientific.
†††††	Shanghai GenePharma, Shanghai, China.
‡‡‡‡‡‡	Lipofectamine 3000, Invitrogen, Thermo Fisher Scientific.

Statistical Analyses

Statistical analysis was performed using Student *t* test or one-way analysis of variance (ANOVA). Statistical methods and *P* values are specified in the relevant figure legend or text. Statistical significance was considered at $P < 0.05$.

RESULTS

Extraction of Human PDLSCs

PDLSCs were isolated and cultured from human samples following established protocols. Flow cytometric analysis was performed to validate the identity of these PDLSCs using antibodies to specific surface molecular markers. Results suggested that these cells were negative for hematopoietic markers CD45 and CD34 but were highly enriched with MSC markers including CD29, CD73, CD90, and CD146 (Fig. 1), confirming effective isolation of human PDLSCs.

Expression of HDAC6 Decreases With PDLSC Aging

In an attempt to identify potential regulators for PDLSC aging, gene expression levels of candidate genes were monitored in different PDLSC-based aging models. DNA damage is an effective inducer for cellular senescence,[23] and senescent PDLSCs were successfully established with etoposide (ETO), a topoisomerase II poison generating single- or double-stranded DNA breaks.[24] Senescence of PDLSCs was confirmed by SA-β-gal staining in ETO-treated but not control cells (Fig. 2A, top panels). Using western blotting and qRT-PCR, significant decrease of HDAC6 expression was detected at both protein and messenger RNA (mRNA) levels in ETO-induced senescent PDLSCs (Fig. 2B). Such expression changes were assessed in an independent senescence model. PDLSCs were continuously cultured for 30 passages in vitro until they entered a morphologic senescent state, validated by SA-β-gal staining (Fig. 2A, bottom panels). Concordantly, western blotting and qRT-PCR demonstrated similar downregulation of HDAC6 in the late and early passage cells (Fig. 2C).

To consolidate this point, PDLSCs were isolated from four donors aged 13, 23, 45, and 63 years, and expression changes of HDAC6 were measured along with chronologic aging. Results indicated that expressions of HDAC6 in PDLSCs from the 45- and 63-year-old donors were significantly lower than in those from the 13- and 23-year-old donors (Fig. 2D, $P < 0.05$; one-way ANOVA).

HDAC6 Inhibition Promotes Senescence and SC Dysfunction in PDLSCs

To test whether reduced HDAC6 function could contribute to aging of PDLSCs and cause deterioration of SC functions in PDLSCs, deacetylase activity of HDAC6 was pharmacologically inhibited by two highly specific inhibitors, rocilinostat and tubastatin A.[25,26] Western blotting confirmed HDAC6 expression was effectively blocked by both agents (Fig. 3A).

These drug-treated PDLSCs were expanded, and their growth was measured by MTT assay. Results

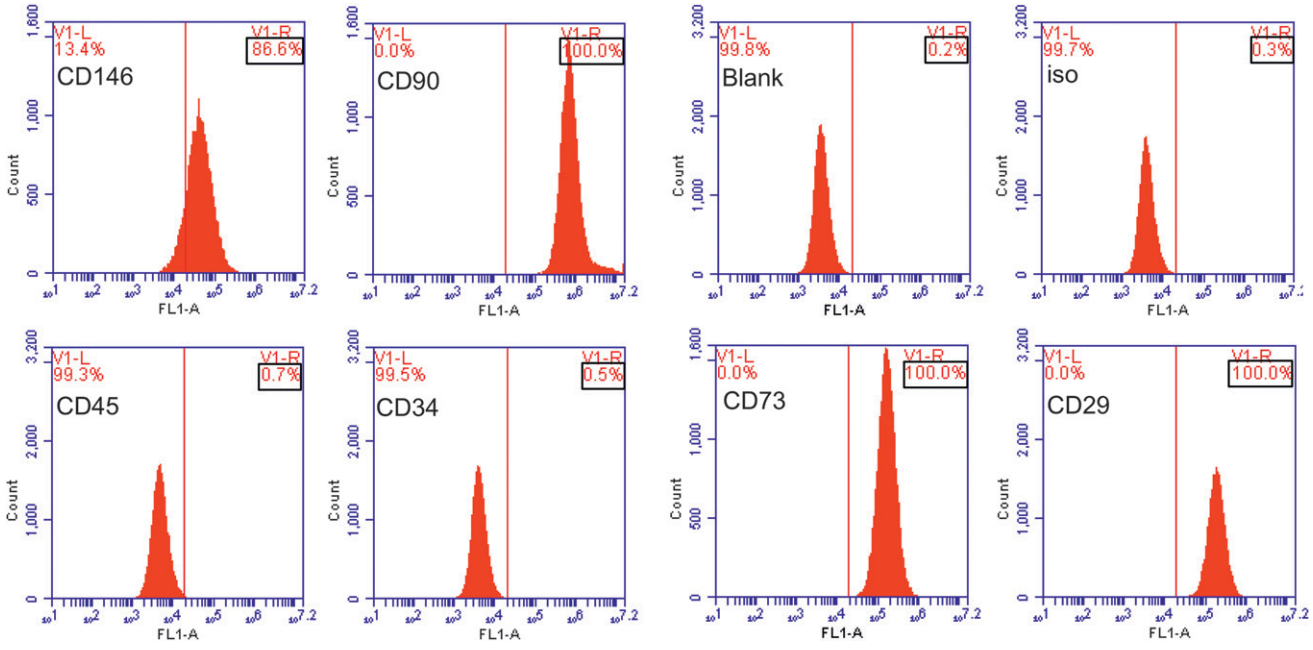

Figure 1.
Cytometric flow analysis of PDLSCs.

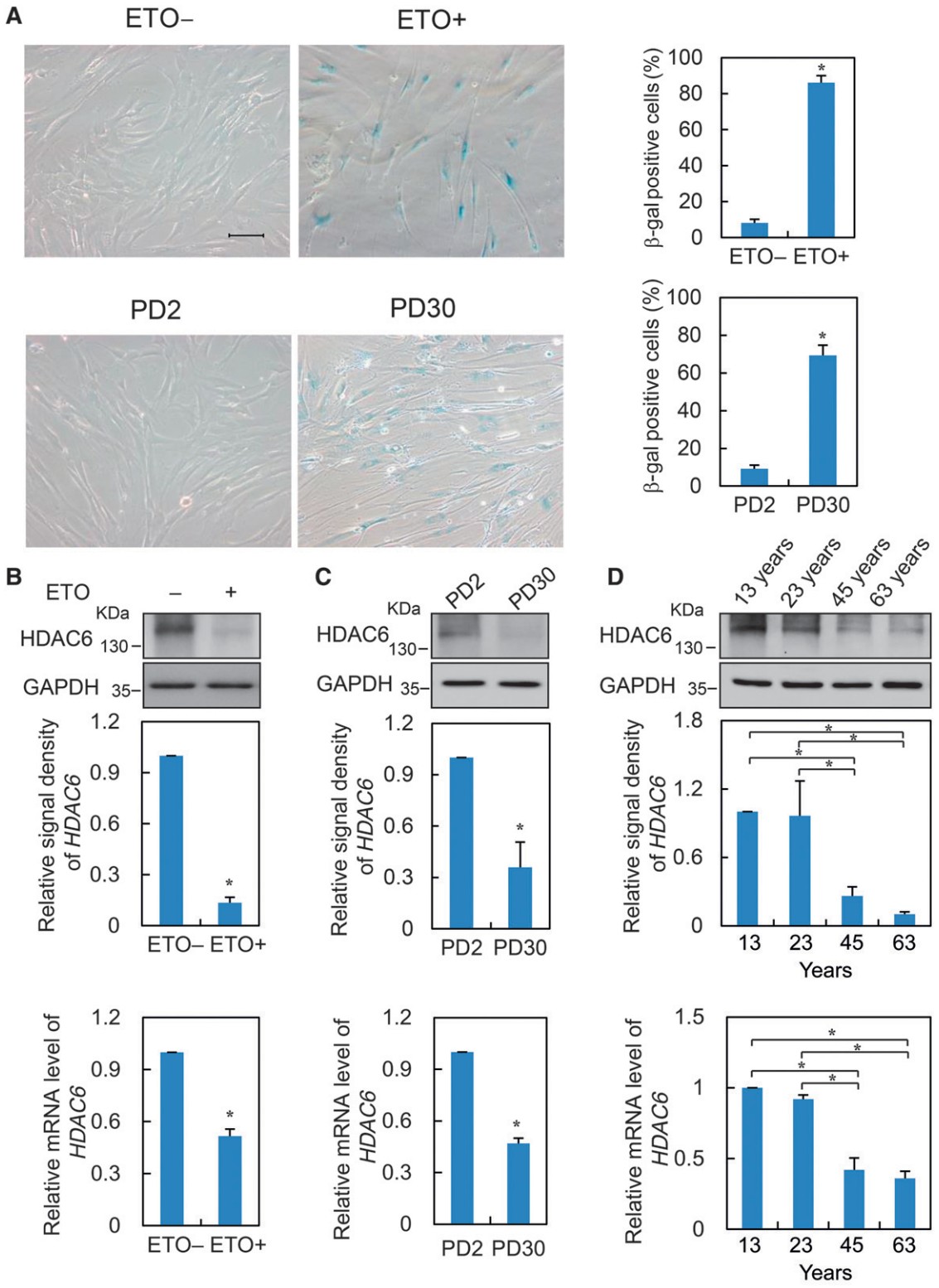

Figure 2.

A) *Representative images of SA-β-gal staining for PDLSCs treated with DMSO (ETO–) or ETO (ETO+) (top), and PDLSCs with population doubling (PD) of 2 or 30 (bottom). Percentage of cells positive for SA-β-gal staining is also shown.* *****P *<0.05; t test. Original magnification ×100; bar = 250 μm. Expression changes of HDAC6 at protein and RNA levels were determined in PDLSCs treated with ETO or vehicle* ***(B)****, in PDLSCs with PD2 or PD30* ***(C)****, and in PDLSCs isolated for 13-, 23-, 45-, and 63-year-old donors* ***(D)****. Western blotting (top) and qRT-PCR (bottom) results are shown.* *****P *<0.05; t test (B, C);* *****P *<0.05; one-way ANOVA (D). Each bar represents mean ± SD for triplicate experiments.*

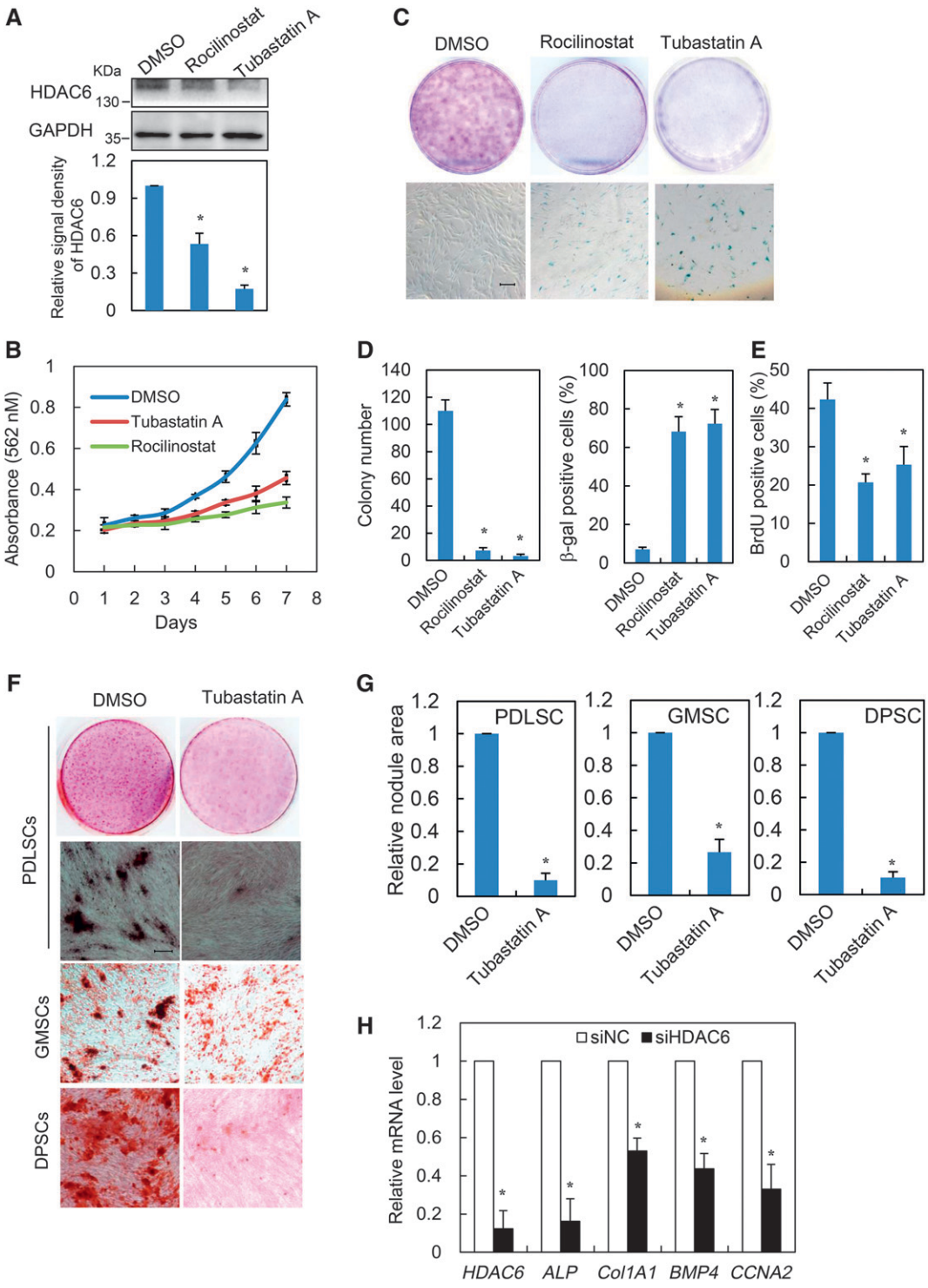

Figure 3.

A) *Protein expression level of HDAC6 in PDLSCs treated with rocilinostat, tubastatin A, or DMSO as control was determined by western blotting.* *******P <0.05; t test. **B)** Growth curves of PDLSCs treated with indicated drugs were determined by MTT assay. Each point represents mean ± SD for triplicate experiments. **C)** Top: PDLSCs treated with indicated drugs were seeded per 30-mm dish for 10 to 15 days followed by fixation and staining with crystal violet. Bottom: PDLSCs treated with indicated drugs were stained for SA-β-gal activity. Original magnification ×40; bar = 500 μm. **D)** Colony number and percentage of SA-β-gal positive cells in Figure 3C;* *******P <0.05; t test. **E)** BrdU incorporation analysis was performed in PDLSCs treated with indicated drugs.* *******P <0.05; t test. Data represent mean ± SD for triplicate experiments. **F)** ARS of cells cultured with indicated drugs 21 days after induction of osteogenic differentiation in PDLSCs, GMSCs, and DPSCs. **G)** Comparison of total areas of mineralized nodules in different groups.* *******P <0.05; t test. Original magnification ×40; bar = 500 μm. **H)** PDLSCs were transfected with siHDAC6 or siNC. Expression of indicated genes was determined using qRT-PCR. Each bar represents mean ± SD for triplicate experiments.* *******P <0.05; t test.

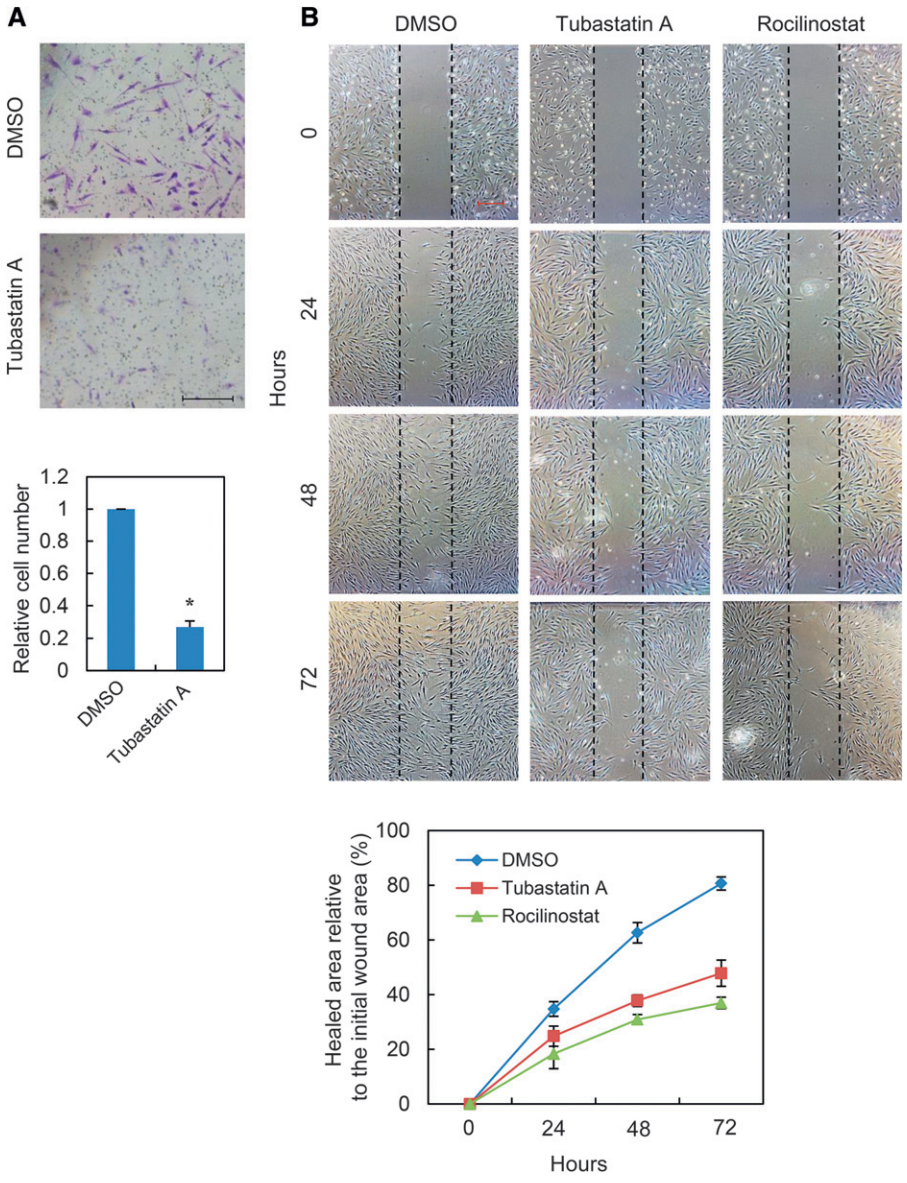

Figure 4.

A) *PDLSCs were treated with DMSO or tubastatin A and subjected to cell invasion assays. Invaded cells were stained with crystal violet and counted.* *****P <0.05; t test. *Original magnification ×100; scale bar = 500 μm.* ***B)*** *The scratch was made on a confluent adherent layer of PDLSCs treated with indicated drugs. Microscopic images were taken at 24-hour intervals during the wound healing process (top). Ratio of healed area at indicated time points relative to initial scratch area are shown as mean ± SD for triplicate experiments. Original magnification ×40; bar = 500 μm.*

indicated that PDLSCs with HDAC6-inhibited by rocilinostat or tubastatin A displayed significantly lower proliferation rate than cells treated with dimethyl sulfoxide (DMSO) as control (Fig. 3B). Such inhibitory effect was further demonstrated using colony formation assay, as limited crystal violet staining of stable clones observed in HDAC6-inhibited cells versus control cells (Figs. 3C and 3D, top and left, respectively). Importantly, characteristic morphologies of senescence, including elevated SA-β-gal activity, enlarged and flattened cell size, and accumulation of granular cytoplasmic inclusions, could be observed in cells treated with rocilinostat or tubastatin A rather than control cells (Figs. 3C and 3D, bottom and right, respectively). Reduced BrdU incorporation supported prosenescence action of rocilinostat and tubastatin A (Fig. 3E).

Application of PDLSC in periodontal regenerative medicine critically depends on its abilities to reconstitute lost periodontal structures such as alveolar bone, PDL, and root cementum, hence necessitating intact and high-efficiency osteogenic differentiation potential from ex vivo expanded PDLSC.[27] Effect of HDAC6 suppression on osteogenic differentiation was tested. HDAC6 was inhibited, and PDLSC senescence was induced with tubastatin A as above, and these PDLSCs were cultured with control cells in osteogenic media to direct osteogenic differentiation. ARS assay results showed that total area of mineralized nodules was significantly decreased in PDLSCs treated with tubastatin A, implying limited osteogenic differentiation when suppressed by HDAC6 (Figs. 3F and 3G). Such an experiment was performed in two other types of dental SCs: GMSCs and DPSCs, which exhibited similar decreased osteogenic differentiation on tubastatin A treatment (Figs. 3F and 3G). Using qRT-PCR analysis with mRNA from PDLSCs transfected with siNC or specific RNA interference (RNAi) against *HDAC6* (siHDAC6), expression levels of osteogenic differentiation markers (*ALP*, *Col1A1*, and *BMP4*[28,29]) and *CCNA2*,[30] a cyclin gene downregulated along with senescence, were examined. In line with phenotypic data, all these genes significantly decreased after *HDAC6* removal (Fig. 3H). These results suggested that suppression of HDAC6 activity or its expression severely impaired osteogenic differentiation potential of dental SCs.

Suppression of HDAC6 Impedes PDLSC Migration

Periodontal regeneration in situ demands local recruitment of naive SCs or progenitors adjacent to a periodontal defect, which migrate and proliferate in response to damaging biologic cues.[27] Effect of HDAC6 inhibition on PDLSC migration, given by critical roles of cytoskeleton in cellular movement, was examined.[31] Transwell assay was performed in PDLSCs treated with tubastatin A. Results indicated that HDAC6-inhibited cells showed much lower migratory capacities than control cells, as fewer cells treated with tubastatin A penetrated the filter (Fig. 4A). In vitro scratch assay was performed in the PDLSC monolayer, and images were captured at 24-hour intervals during PDLSC migration to close the scratch. HDAC6 inhibition by tubastatin A or rocilinostat greatly suppressed PDLSC movement, which was most obvious 48 hours after creation of the scratch (Fig. 4B). Therefore, data implied that HDAC6 inhibition negatively regulates migratory activity of PDLSCs along with cells approaching senescence.

Suppression of HDAC6 Activates p27^{Kip1}

A hallmark of senescence is the stable and long-term loss of proliferation for primary cells during in vitro culturing.[5] Such cell cycle arrest is mechanistically associated with activation of key tumor suppressors, including p53/p21^{Cip1}, p16^{INK4a}, and p27^{Kip1}.[5,21,32] Expression patterns of p16^{INK4a}, p21^{Cip1}, and p27^{Kip1} were analyzed by western blotting during HDAC6-mediated PDLSC aging. As shown in Figure 5A, protein levels of p27^{Kip1} progressively elevated when PDLSC was treated with increasing dosages of tubastatin A, whereas protein levels of p16^{INK4a} and p21^{Cip1} remained unchanged. qRT-PCR analyses demonstrated mRNA levels of all three genes were nearly unaffected in cells treated with tubastatin A (Fig. 5B). Elevated protein levels of p27^{Kip1} in HDAC6-depleted PDLSCs were observed when using sequence-specific RNAi against *HDAC6* (Fig. 5C). These results imply that suppression of HDAC6 promotes PDLSC aging probably by upregulating or stabilizing p27^{Kip1} posttranscriptionally.

HDAC6 Interacts With p27^{Kip1} and Regulates p27^{Kip1} Acetylation

To gain mechanistic insights into posttranscriptional regulation of p27^{Kip1} by HDAC6, p27^{Kip1} association with HDAC6 was examined. Physical interaction between endogenous p27^{Kip1} and HDAC6 was validated using antibodies against p27^{Kip1} in PDLSCs (Fig. 6A, top panel). Reciprocal CoIP with antibodies against HDAC6 also confirmed their interaction in PDLSCs (Fig. 6A, bottom panel). This point was strengthened with their evident interaction in GMSCs and DPSCs (Fig. 6B).

In view of intrinsic enzymatic activities of HDAC6, the possibility that p27^{Kip1} could be deacetylated by HDAC6 was tested. HEK293 cells were transfected with FLAG-p27^{Kip1}, and cells were treated with tubastatin A or rocilinostat to inhibit deacetylase activities of HDAC6. FLAG-p27^{Kip1} was purified by FLAG-M2 resin and eluted from beads with excessive competitive FLAG peptide. Acetylation state of p27^{Kip1} was measured by western blotting using antibodies against pan-acetylation. With comparable p27^{Kip1} enriched by this method, significantly increased acetylation was observed when HDAC6 was inhibited by either agent (Fig. 6C). Concordantly, interaction between p27^{Kip1} and HDAC6 was severely impaired in

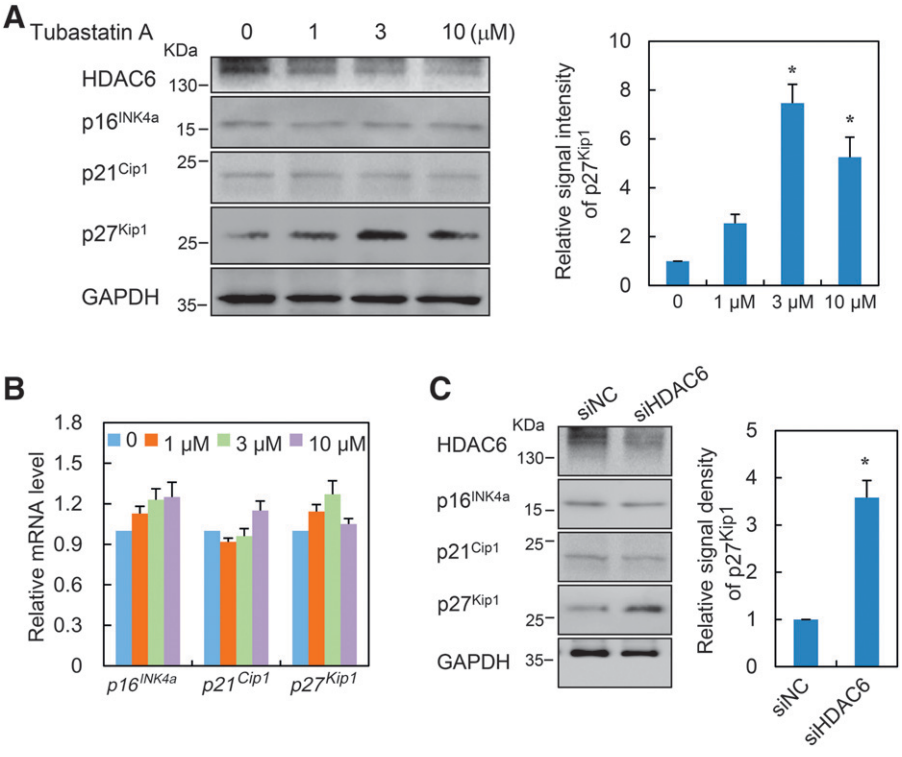

Figure 5.

Total protein and RNA expression of indicated SA genes by western blotting ***(A)*** *and qRT-PCR* ***(B)****.* *******P <0.05; t test. **C)** PDLSCs transfected with siHDAC6 or siNC were harvested for western blotting assay to probe the expression pattern of p27^{Kip1}. GAPDH served as loading control.* *******P <0.05; t test. Each bar represents mean ± SD for triplicate experiments.*

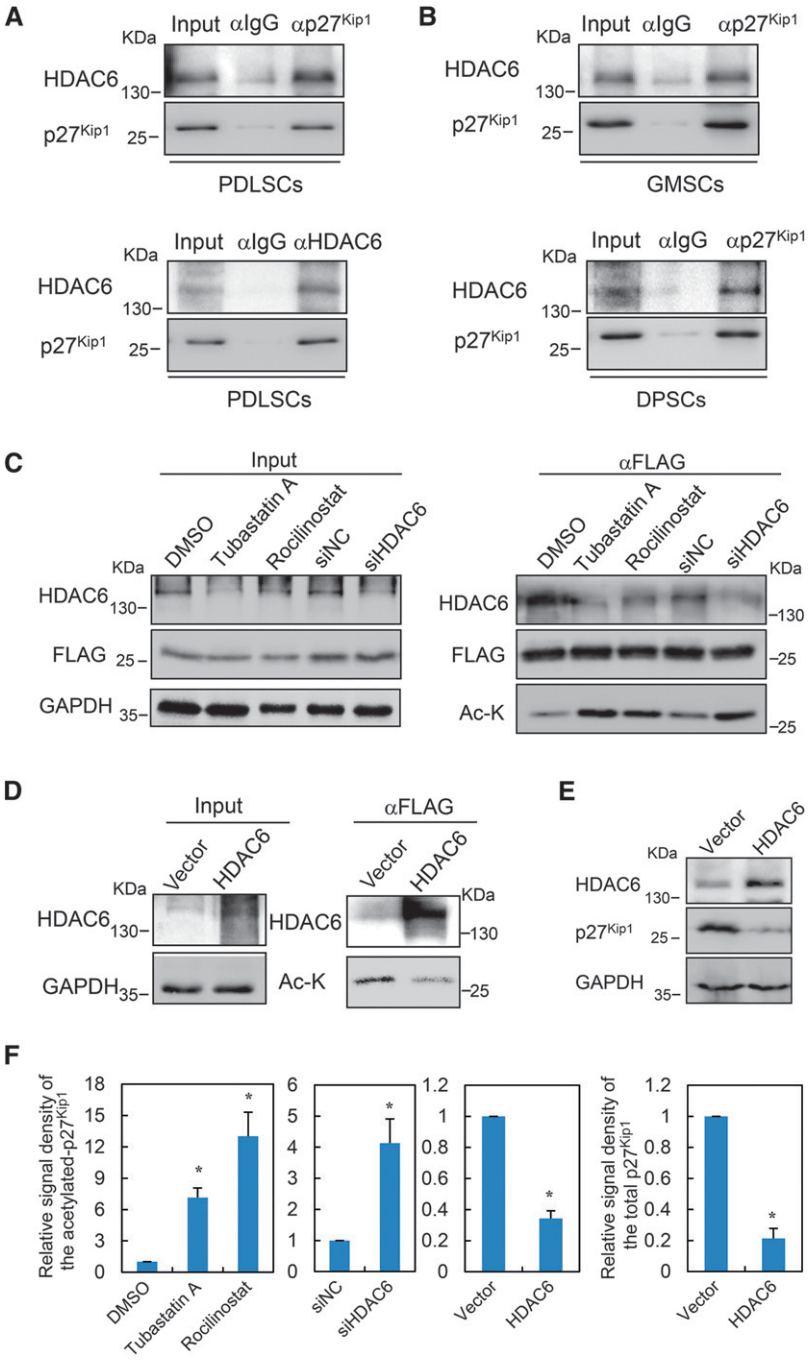

Figure 6.

A) *CoIP was performed in PDLSCs with antibodies against p27^{Kip1} (top) or HDAC6 (bottom). Precipitated complex was resolved on sodium dodecyl sulfate-polyacrylamide gel electrophoresis and blotted with indicated antibodies.* ***B)*** *CoIP assay as in Figure 6A was performed with p27^{Kip1} antibody in GMSCs (top) and DPSCs (bottom).* ***C)*** *HEK293 cells transfected with FLAG-tagged p27^{Kip1} were challenged with HDAC6 loss-of-function either by pharmacologic inhibition using tubastatin A or rocilinostat or by RNAi-mediated knockdown. Cell extracts were subjected to CoIP assay using anti-FLAG resin. Levels of FLAG-tagged p27^{Kip1} and acetylated p27^{Kip1} were analyzed by western blotting using anti-FLAG and antipan-acetylation (Ac-K) antibodies, respectively.* ***D)*** *Plasmid for HDAC6 expression or control vector was cotransfected with FLAG-tagged p27^{Kip1} in HEK293 cells. Cell lysate was subjected to CoIP assay and western blotting analysis as in panel C.* ***E)*** *Whole cell lysate from HEK293 cells transfected with HDAC6 or control vector was subjected to western blotting analysis.* ***F)*** *Relative signal densities of acetylated-p27^{Kip1} in Figures 6C and 6D or total p27^{Kip1} in Figure 6E were quantified and are shown as mean ± SD for triplicate experiments.* ******** *P <0.05; t test.*

HDAC6-inhibited cells (Fig. 6C). Using RNAi-based knockdown of *HDAC6*, increased acetylation of p27^{Kip1} and decreased interaction between HDAC6 and p27^{Kip1} were observed in *HDAC6*-depleted cells compared with control cells (Fig. 6C). To further consolidate this observation, HDAC6 was overexpressed, and significantly decreased p27^{Kip1} acetylation was found on HDAC6 overexpression (Fig. 6D). Ectopic expression of HDAC6 also resulted in downregulation of p27^{Kip1} proteins (Fig. 6E). Statistical analyses in Figure 6F quantified the inverse regulation of p27^{Kip1} acetylation or total protein level by HDAC6 as in Figures 6C through 6E. Together with data in Figure 5, these results suggest that p27^{Kip1} is a novel substrate of HDAC6 and its cytoplasmic stability is regulated by HDAC6-dependent deacetylation.

DISCUSSION

Circumvention from time-dependent functional decline of SCs in chronologic aging and ex vivo culturing is crucial for availability of SCs in tissue regeneration.[1] Despite the expectation of autologous PDLSC-based therapeutics for periodontal regeneration, incomplete formation of new bone and cementum at denuded root surfaces is often observed in aged donors with decreased matrix content and exhausted proliferation.[15,33] Hence, identification of a maneuverable target of PDLSC aging demands control of such functional decay. Recently, Vozzi et al.[34] found that p16^{INK4a} and p53 were involved in replicative senescence of periosteum-derived progenitor cells. In the current study, HDAC6 was characterized as a novel target in aging of PDLSCs, and its expressional decline and functional causality were validated in this process.

HDAC6 is distinguished from other HDACs owing to its unique cytoplasmic localization and tubulin deacetylase activity that has effects on a broad class of cellular functions mediated by microtubules.[35,36] Of them, HDAC6-associated regulation of proteostasis and apoptosis is critically connected with aging and is defined as a hallmark therein.[1] This aspect of regulation merits further investigations in the aged condition. This study focuses on migration and unexplored osteogenic differentiations regulated by HDAC6, given by their direct and crucial implications in PDLSC-based periodontal regeneration. Severely impaired transwell invasion and low-efficient closure of the scratch by inhibition of HDAC6 deacetylase activity, which was accompanied by downregulated BMP4 mRNA levels, were observed. These findings resemble results from transforming growth factor β1-mediated epithelial–mesenchymal transition in a tumor microenvironment, reflecting necessity of HDAC6-dependent deacetylation of α-tubulin for cell motility and invasiveness.[37] In this regard, overexpression of HDAC6 leads to global deacetylation of α-tubulin and promotes chemotactic cell movement.[36] Indeed, impediments to mobility of PDLSCs suppress their responsiveness to mechanoinduction and other physical stimuli and affect healing and regeneration of damaged cells.[38,39] In line with this, aged MSCs were described as possessing a less dynamic cytoskeleton and lower migratory speed with fewer cells capable of homing to site of injury, leading to a decrease in regeneration capacity;[15] accordingly, data from the current study suggested key roles of HDAC6 in this process.

Lineage specification of naive MSCs is extremely sensitive to tissue-level elasticity.[40] A recent study highlighted the role of stiffness in triggering expression of osteogenic genes.[41] It is reported that soft matrices mimicking the brain direct neurogenic differentiation of MSCs; much higher stiffness is obligated for its commitment to osteoblasts.[40] In view of this notion, computational analysis on a cell tensegrity model indicated that microtubules function as compression-supporting elements to balance tension raised from actomyosin contraction and consequently determine maximal cell sensitivity to stiffness in mechanotransduction.[42] It is conceivable that HDAC6 regulates osteogenic commitment of PDLSCs both by maintenance of appropriate cytoskeleton organization and by its adaption to different mechanical signals. Osteogenic differentiation was found to be greatly impaired after inhibition of deacetylase activity of HDAC6.

Despite the complexity of diverse causes of aging, including toxic metabolites, genomic instability, mitochondrial dysfunction, and telomere attrition,[1] these converge during aging on the clock for cell proliferation and individually or cooperatively arrest the cell cycle. Interestingly, in the current study, cell cycle regulator $p27^{Kip1}$ but not p53, $p16^{INK4a}$, or $p21^{Cip1}$ is specifically upregulated or stabilized in aging models associated with HDAC6 inhibition. Lack of mRNA level change of $p27^{Kip1}$ implied posttranscriptional regulation of $p27^{Kip1}$ by HDAC6 in PDLSC aging. Data from this study validated this possibility, showing their physical interaction and elevated $p27^{Kip1}$ acetylation when HDAC6 was suppressed by drugs or siRNA-mediated knockdown. HDAC6-asscociated deacetylation of $p27^{Kip1}$ has no connection with acetylation of nuclear $p27^{Kip1}$ as shown in a previous report.[43] Nuclear $p27^{Kip1}$ is a component of a transcriptional coregulator complex and is acetylated by p300/CREB binding protein associated factor in its K100 residue, which induces degradation of $p27^{Kip1}$ by proteasome.[43] Suppression of HDAC6, localized exclusively in the cytoplasm,[36] enhances its stability, implying acetylation of cytoplasmic $p27^{Kip1}$ might be catalyzed by another acetyltransferase, and this modification is a stabilizer contrary to its roles in the nucleus. Although it is possible that HDAC6 regulates proliferation exhaustion of PDLSCs through indirect routes, identification of $p27^{Kip1}$ as its substrate expanded knowledge on pathways intersecting with HDAC6 and also added another function in HDAC6-involved cancer biology.[44]

CONCLUSION

Data suggest that HDAC6 orchestrates proliferation, mobility, and osteogenic differentiation of PDLSCs, which is impaired along with decreased HDAC6 expression during aging of PDLSCs.

ACKNOWLEDGMENTS

The authors are grateful to Prof. Xiaomei Liao (School of Life Science, Central China Normal University, Wuhan, China) for providing the pcDNA3.1-HDAC6 plasmid. The authors also thank Dr. Yu Zhang (Peking University Health Science Center, Beijing, China) for helpful proposal and stimulating discussion. This work was supported by the International Science & Technology Cooperation Program of China (#2015DFB30040) to Yunyan Zhu, and the National Natural Science Foundation of China (#81470717 to Yunyan Zhu and # 81502345 to Qian Li. The authors report no conflicts of interest related to this study.

REFERENCES

1. López-Otín C, Blasco MA, Partridge L, Serrano M, Kroemer G. The hallmarks of aging. *Cell* 2013;153: 1194-1217.
2. Signer RA, Morrison SJ. Mechanisms that regulate stem cell aging and life span. *Cell Stem Cell* 2013;12: 152-165.

3. Sethe S, Scutt A, Stolzing A. Aging of mesenchymal stem cells. *Ageing Res Rev* 2006;5:91-116.
4. Rauscher FM, Goldschmidt-Clermont PJ, Davis BH, et al. Aging, progenitor cell exhaustion, and atherosclerosis. *Circulation* 2003;108:457-463.
5. Kuilman T, Michaloglou C, Mooi WJ, Peeper DS. The essence of senescence. *Genes Dev* 2010;24:2463-2479.
6. Hong H, Takahashi K, Ichisaka T, et al. Suppression of induced pluripotent stem cell generation by the p53-p21 pathway. *Nature* 2009;460:1132-1135.
7. Li H, Collado M, Villasante A, et al. p27(Kip1) directly represses Sox2 during embryonic stem cell differentiation. *Cell Stem Cell* 2012;11:845-852.
8. Li H, Collado M, Villasante A, et al. The Ink4/Arf locus is a barrier for iPS cell reprogramming. *Nature* 2009;460:1136-1139.
9. Seo BM, Miura M, Gronthos S, et al. Investigation of multipotent postnatal stem cells from human periodontal ligament. *Lancet* 2004;364:149-155.
10. Huang CY, Pelaez D, Dominguez-Bendala J, Garcia-Godoy F, Cheung HS. Plasticity of stem cells derived from adult periodontal ligament. *Regen Med* 2009;4:809-821.
11. Lin NH, Gronthos S, Bartold PM. Stem cells and future periodontal regeneration. *Periodontol 2000* 2009;51:239-251.
12. Yoshida T, Washio K, Iwata T, Okano T, Ishikawa I. Current status and future development of cell transplantation therapy for periodontal tissue regeneration. *Int J Dent* 2012;2012:307024.
13. Hynes K, Menicanin D, Gronthos S, Bartold PM. Clinical utility of stem cells for periodontal regeneration. *Periodontol 2000* 2012;59:203-227.
14. Chen FM, Sun HH, Lu H, Yu Q. Stem cell-delivery therapeutics for periodontal tissue regeneration. *Biomaterials* 2012;33:6320-6344.
15. Zhang J, An Y, Gao LN, Zhang YJ, Jin Y, Chen FM. The effect of aging on the pluripotential capacity and regenerative potential of human periodontal ligament stem cells. *Biomaterials* 2012;33:6974-6986.
16. Konstantonis D, Papadopoulou A, Makou M, Eliades T, Basdra EK, Kletsas D. Senescent human periodontal ligament fibroblasts after replicative exhaustion or ionizing radiation have a decreased capacity towards osteoblastic differentiation. *Biogerontology* 2013;14:741-751.
17. Haberland M, Montgomery RL, Olson EN. The many roles of histone deacetylases in development and physiology: Implications for disease and therapy. *Nat Rev Genet* 2009;10:32-42.
18. Seidel C, Schnekenburger M, Dicato M, Diederich M. Histone deacetylase 6 in health and disease. *Epigenomics* 2015;7:103-118.
19. Iwata T, Yamato M, Zhang Z, et al. Validation of human periodontal ligament-derived cells as a reliable source for cytotherapeutic use. *J Clin Periodontol* 2010;37:1088-1099.
20. Zheng W, Wang S, Ma D, Tang L, Duan Y, Jin Y. Loss of proliferation and differentiation capacity of aged human periodontal ligament stem cells and rejuvenation by exposure to the young extrinsic environment. *Tissue Eng Part A* 2009;15:2363-2371.
21. Li Q, Zhang Y, Fu J, et al. FOXA1 mediates p16(INK4a) activation during cellular senescence. *EMBO J* 2013;32:858-873.
22. Pittenger MF, Mackay AM, Beck SC, et al. Multilineage potential of adult human mesenchymal stem cells. *Science* 1999;284:143-147.
23. Fumagalli M, Rossiello F, Clerici M, et al. Telomeric DNA damage is irreparable and causes persistent DNA-damage-response activation. *Nat Cell Biol* 2012;14:355-365.
24. Nitiss JL. Targeting DNA topoisomerase II in cancer chemotherapy. *Nat Rev Cancer* 2009;9:338-350.
25. Santo L, Hideshima T, Kung AL, et al. Preclinical activity, pharmacodynamic, and pharmacokinetic properties of a selective HDAC6 inhibitor, ACY-1215, in combination with bortezomib in multiple myeloma. *Blood* 2012;119:2579-2589.
26. Butler KV, Kalin J, Brochier C, Vistoli G, Langley B, Kozikowski AP. Rational design and simple chemistry yield a superior, neuroprotective HDAC6 inhibitor, tubastatin A. *J Am Chem Soc* 2010;132:10842-10846.
27. Chen FM, Zhang J, Zhang M, An Y, Chen F, Wu ZF. A review on endogenous regenerative technology in periodontal regenerative medicine. *Biomaterials* 2010;31:7892-7927.
28. Cheng H, Jiang W, Phillips FM, et al. Osteogenic activity of the fourteen types of human bone morphogenetic proteins (BMPs). *J Bone Joint Surg Am* 2003;85-A:1544-1552.
29. Luu HH, Song WX, Luo X, et al. Distinct roles of bone morphogenetic proteins in osteogenic differentiation of mesenchymal stem cells. *J Orthop Res* 2007;25:665-677.
30. Narita M, Nũnez S, Heard E, et al. Rb-mediated heterochromatin formation and silencing of E2F target genes during cellular senescence. *Cell* 2003;113:703-716.
31. Valenzuela-Fernández A, Cabrero JR, Serrador JM, Sánchez-Madrid F. HDAC6: A key regulator of cytoskeleton, cell migration and cell-cell interactions. *Trends Cell Biol* 2008;18:291-297.
32. Alexander K, Hinds PW. Requirement for p27(KIP1) in retinoblastoma protein-mediated senescence. *Mol Cell Biol* 2001;21:3616-3631.
33. Wu RX, Bi CS, Yu Y, Zhang LL, Chen FM. Age-related decline in the matrix contents and functional properties of human periodontal ligament stem cell sheets. *Acta Biomater* 2015;22:70-82.
34. Vozzi G, Lucarini G, Dicarlo M, et al. In vitro lifespan and senescent behaviour of human periosteal derived stem cells. *Bone* 2016;88:1-12.
35. Li Y, Shin D, Kwon SH. Histone deacetylase 6 plays a role as a distinct regulator of diverse cellular processes. *FEBS J* 2013;280:775-793.
36. Hubbert C, Guardiola A, Shao R, et al. HDAC6 is a microtubule-associated deacetylase. *Nature* 2002;417:455-458.
37. Shan B, Yao TP, Nguyen HT, et al. Requirement of HDAC6 for transforming growth factor-beta1-induced epithelial-mesenchymal transition. *J Biol Chem* 2008;283:21065-21073.
38. Ng TK, Huang L, Cao D, et al. Cigarette smoking hinders human periodontal ligament-derived stem cell proliferation, migration and differentiation potentials. *Sci Rep* 2015;5:7828.
39. Ruiz JP, Pelaez D, Dias J, Ziebarth NM, Cheung HS. The effect of nicotine on the mechanical properties of mesenchymal stem cells. *Cell Health Cytoskelet* 2012;4:29-35.

40. Engler AJ, Sen S, Sweeney HL, Discher DE. Matrix elasticity directs stem cell lineage specification. *Cell* 2006;126:677-689.
41. Mattei G, Ferretti C, Tirella A, Ahluwalia A, Mattioli-Belmonte M. Decoupling the role of stiffness from other hydroxyapatite signalling cues in periosteal derived stem cell differentiation. *Sci Rep* 2015;5: 10778.
42. De Santis G, Lennon AB, Boschetti F, Verhegghe B, Verdonck P, Prendergast PJ. How can cells sense the elasticity of a substrate? An analysis using a cell-tensegrity model. *Eur Cell Mater* 2011;22:202-213.
43. Pérez-Luna M, Aguasca M, Perearnau A, et al. PCAF regulates the stability of the transcriptional regulator and cyclin-dependent kinase inhibitor p27 Kip1. *Nucleic Acids Res* 2012;40:6520-6533.
44. Aldana-Masangkay GI, Sakamoto KM. The role of HDAC6 in cancer. *J Biomed Biotechnol* 2011;2011: 875824.

Correspondence: Dr. Yanheng Zhou, Department of Orthodontics, School and Hospital of Stomatology, Peking University, 22 Zhongguancun South Ave., Beijing 100081, China. Fax: 86-10-62173402; e-mail: yanhengzhou@vip.163.com.

Submitted May 27, 2016; accepted for publication July 30, 2016.